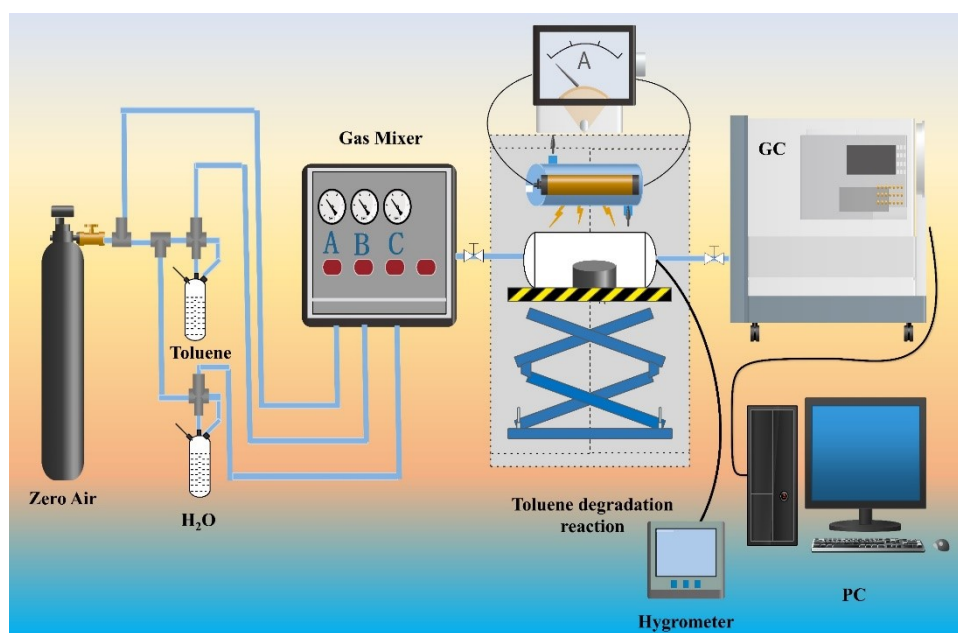


## Supporting Information

### 3D structured TiO<sub>2</sub>-based aerogel photocatalyst for high-efficiency degradation of toluene gas

Li Zhang<sup>\*a,§</sup>, Li Dai<sup>a,§</sup>, Xueying Li<sup>a</sup>, Wei Yu<sup>a</sup>, Shijie Li<sup>b</sup>, and Jie Guan<sup>\*a</sup>

#### Photocatalytic activity measurements



**Fig. S1.** Schematic diagram of photocatalytic degradation experimental device.

#### Synthesis of the 3D Zr/TiO<sub>2</sub>/SiO<sub>2</sub> composite aerogels:

As a sample for comparison, the synthesis of the 3D Zr/TiO<sub>2</sub>/SiO<sub>2</sub> composite aerogels was according to the published literature [1]. Generally, the TiO<sub>2</sub> precursor solution was prepared as the same as 2.2. Then, 0.9 g of zirconium acetate is added into 16.2 ml TiO<sub>2</sub> precursor solution, and Zr/TiO<sub>2</sub> nanofibers are obtained by electrospinning and high-temperature calcination method. Then, 5 g of ethyl orthosilicate, 45 g of ethanol, 20 g of deionized water, and 0.02 g of phosphoric acid were mixed for 2 h to obtain SiO<sub>2</sub> sol. The obtained SiO<sub>2</sub> sol and Zr/TiO<sub>2</sub> nanofibers are uniformly mixed, transferred to a mold, and quickly frozen in liquid nitrogen. Finally, the above products are freeze-dried to obtain Zr/TiO<sub>2</sub>/SiO<sub>2</sub> aerogel.

## BET Analysis

Fig. S2 shows the N<sub>2</sub> adsorption-desorption isotherm and the corresponding pore size distribution curve (inset) of the samples. All the samples show type IV isotherms and type H3 hysteresis loops. It is generally believed that H3 hysteresis loops are slit holes formed by the accumulation of flake particles [2]. The pore size distribution curves show that all the three samples of RGO, TiO<sub>2</sub>, and PTA have a large number of mesopores, while PTA also has some micropores. Furthermore, a Brunauer–Emmett–Teller (BET) analysis displayed that the surface area of RGO, TiO<sub>2</sub>, and PTA were 258.838, 53.971, and 498.442 m<sup>2</sup>/g, respectively. The high specific surface area of PTA is conducive to enriching more pollutants, increasing the contact area between pollutants and the catalyst, and generating more photocatalytic active sites, thereby producing excellent photocatalytic performance.

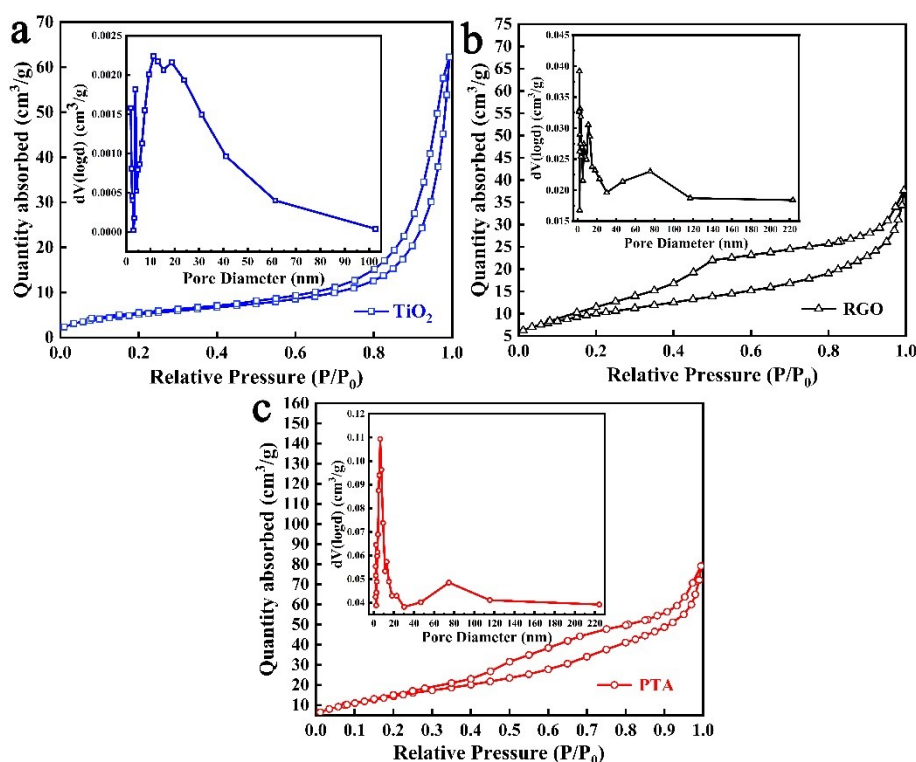


**Fig. S2.** N<sub>2</sub> adsorption–desorption isotherm and the corresponding pore size distribution curves (inset) of the samples.

## Contact angle test

As shown in Fig. S3, the contact angle of water droplets on the surface of TiO<sub>2</sub> is almost 0°, while the contact angle of oil droplets on its surface is 117°. It can be seen

that  $\text{TiO}_2$  is a hydrophilic and oleophobic substance. Whether the pollutant molecules are liquid or gaseous, they must be adsorbed from the fluid to the surface of the photocatalyst before they can be photocatalytically degraded. Therefore, hydrophilic  $\text{TiO}_2$  is not conducive to photocatalytic degradation of non-polar organic pollutants. The coupling of RGO has solved the above problem, as the contact angle of the oil droplets on the surface of the 3D PTA is almost  $0^\circ$ . The improvement of lipophilicity is more conducive to enhancing the removal efficiency of non-polar pollutants by the composite aerogel. This provides a prerequisite for improving the efficiency of 3D PTA photocatalytic degradation of toluene.

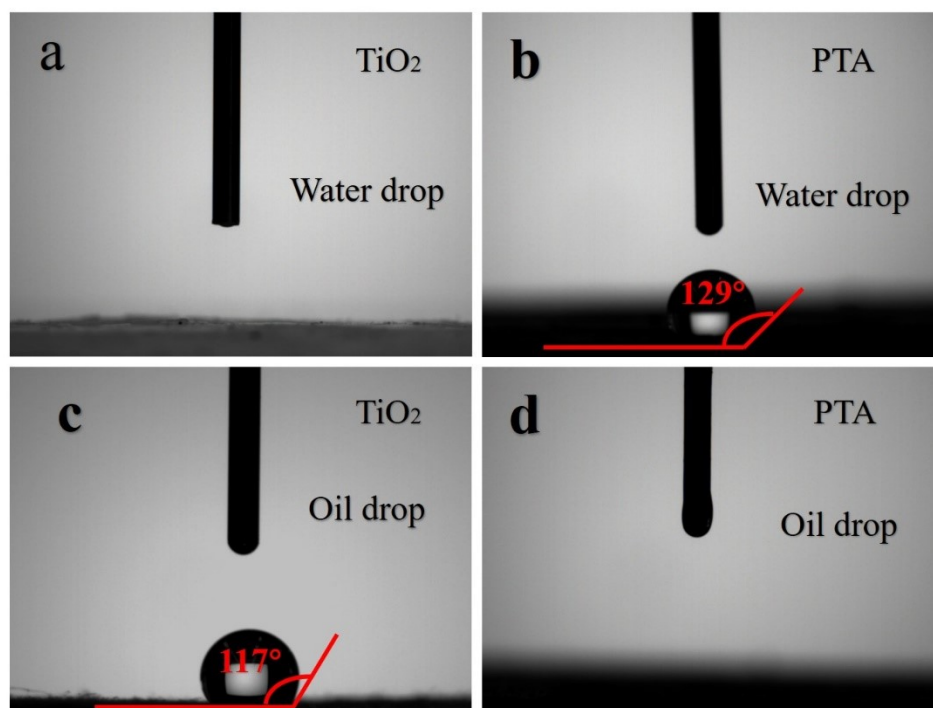


**Fig. S3.** Photograph of the wettability of water droplets on (a)  $\text{TiO}_2$  nanofibers, (b) PTA and oil drop on (c)  $\text{TiO}_2$  nanofiber and (d) PTA.

In order to compare this work with the reported literatures, we summarized and calculated the remove efficiency of toluene ( $\text{ppm}\cdot\text{min}^{-1}$ ), as shown in Fig. S4, Supporting Information. It can be seen that this work has made progress in terms of initial concentration and photocatalytic efficiency comparing with others' work [3-8].

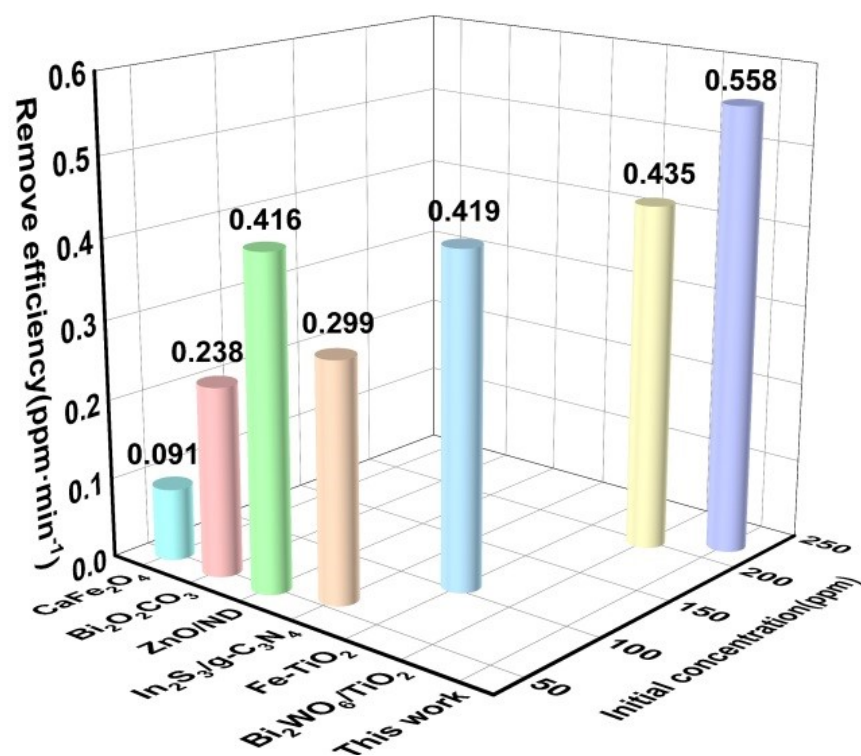


Fig. S4. Performance comparison between this work and others.

## References

- [1] M. Zhang, Y. Wang, Y. Zhang, J. Song, Y. Si, J. Yan, C. Ma, Y.T. Liu, J. Yu, B. Ding, *Angew. Chem. Int. Ed. Engl.* 2020, 59, 23252-23260.
- [2] L. Zhang, P. Ma, L. Dai, S. Li, W. Yu, J. Guan, *Catal. Sci. Technol.* 2021, 11, 3834-3844.
- [3] J. Ding, H. Wang, Y. Luo, Y. Xu, J. Liu, Y. Lin, *Catalysts*, 2020,10, 389-403.
- [4] M. Zhang, X. Liu, X. Zeng, M. Wang, J. Shen, R. Liu, *Chem. Phys. Lett.*, 2020,738, 100094.
- [5] Z. Yin, B. Liu, S. Fan, P. Wang, X. Wang, D. Long, L. Zhang, X. Yang, X. Li, *Catal. Commun.*, 2019,130, 105754.
- [6] Z. Sun, J. Fan, R. Feng, M. Wang, Y. Zhou, L. Zhang, *Journal of Chemical Technology & Biotechnology*, 2021,96, 1732-1741.
- [7] G. Zeng, Q. Zhang, Y. Liu, S. Zhang, J. Guo, *Nanomaterials (Basel)*, 2019,9, 1773-1790.
- [8] J. Liu, P. Wang, W. Qu, H. Li, L. Shi, D. Zhang, *Appl. Catal., B.*, 2019,257, 117880.